Image Cover Sheet

CLASSIFICATION	SYSTEM NUMBER
UNCLASSIFIED	513095

TITLE

Analysis of Reverse Dive Profiles Using the DCIEM Bubble Evolution Model. Part I: Model Development

System Number:

Patron Number:

Requester:

Notes:

DSIS Use only:

Deliver to:

SL 1999-123

ANALYSIS OF REVERSE DIVE PROFILES USING THE DCIEM BUBBLE EVOLUTION MODEL PART I: MODEL DEVELOPMENT

Peter Tikuisis
Ron Y. Nishi
Defence & Civil Institute of Environmental Medicine
1133 Sheppard Avenue West, PO Box 200
Toronto, ONTARIO, M3M 3B9 CANADA

The DCIEM bubble evolution model, calibrated against Doppler-detected bubble scores, is used to calculate the growth and decay of bubbles generated by a dive/decompression profile. The maximum bubble radius attained can be used as a measure of the risk of decompression sickness. Application of the model to reverse dive profiles suggests that these profiles do not present a markedly higher risk of DCS compared to conventional repetitive profiles.

Introduction

The DCIEM bubble evolution model, calibrated against Doppler-detected bubble scores, is used to calculate the growth and decay of bubbles generated by a dive/decompression profile. The maximum bubble radius attained can be used as a measure of the risk of decompression sickness (DCS). In Part 1, we outline the development of the model and compare its prediction to the risk of DCS for a wide range of dive profiles.

Model Development and Calibration

The bubble evolution model originated from an investigation to correlate bubble incidence in divers to a probabilistic model prediction of bubble evolution (Gault *et al.*, 1995). The bubble model incorporates a finite inert gas availability constraint for the formation of the bubble, perfusion-limitation of gas exchange between the blood and tissue, and a gas diffusion barrier at the bubble boundary. The method of maximum likelihood was applied to the original model against bubble grade data based on the Kisman-Masurel classification of Doppler-detected bubbles (Nishi, 1993). The data were comprised of 2,064 man-dives involving 276 air and 86 heliox dives. Air dives included single and repetitive exposures, standard decompression dives, dives with oxygen decompression at 9 msw, and surface decompression dives involving surfacing from 9 msw and recompressing back to 12 msw to complete the decompression. Heliox dives were mostly 84% He:16% O_2 with air decompression to 9 msw followed by O_2 decompression at 9 msw.

Maximum bubble grade data were used for the model calibration of the maximum bubble size (R_{max}) predicted. Bubble grades were categorized according to no bubbles detected (42.5% of cases), light bubble activity (BG's of 1 and 2; 28.1%), and heavy bubble activity (BG's of 3 and 4; 29.4%). Key model parameters fitted by maximum likelihood included the time constants of N_2 and He (τ_{N2} and τ_{He}, respectively), the gas flux coefficient at the bubble boundary (k_{N2} and k_{He}, where gas flux = $k \cdot \Delta conc$), and the Ostwald gas solubility coefficient in the tissue compartment (L_{N2} and L_{He}). Subsequently, the model has been expanded (Nishi *et al.*, 1997) to include two compartments and calibrated against a larger data set (original plus 464 nitrox man-dives). The resultant percentages of BG cases were 44.0% (0), 28.3% (1, 2), and 27.7% (3, 4). Common to both model compartments are the tissue volume (10^{-4} mL), tissue surface tension (30 dyne·cm^{-1}), H_2O vapor tension (0.0619 atm), and CO_2 or metabolic gas tension (0.0625 atm). The estimated parameters are listed in the table below.

Table 1: Bubble model parameter estimates; τ = time constant; k = bubble boundary gas flux rate coefficient; and L = Ostwald gas solubility coefficient.

Parameter	Compartment 1		Compartment 2	
	N_2	He	N_2	He
τ (min)	27.8	21.7	158.9	72.0
k ($cm \cdot s^{-1}$)	7.033×10^{-3}	1.690×10^{-2}	4.639×10^{-3}	11.839×10^{-2}
L	0.0215	0.0110	0.0463	0.0138

Figure 1 shows the predicted bubble evolution in both model compartments for a standard air decompression dive (150 fsw for 30 min). In this example, the predicted bubble formation for the 2nd compartment lags the formation in the 1st compartment because of a lower gas tension. However, the subsequent growth of the bubble in the 2nd compartment after further decompression is larger because of a longer retention of the excess gas tension.

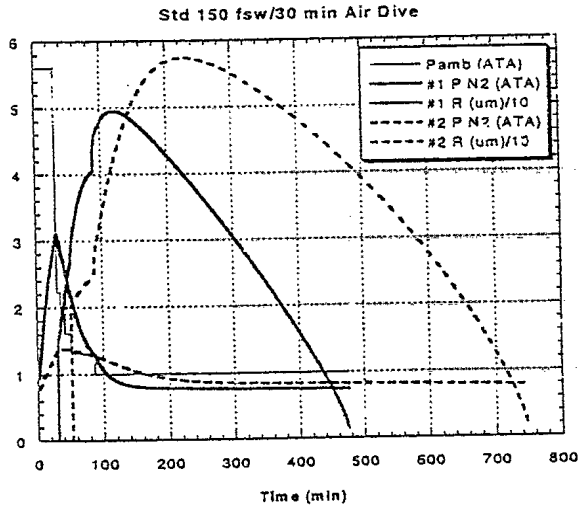

Fig. 1. Predicted N_2 tension and bubble evolution in the two model compartments for a 150 fsw/30 min air dive.

It is emphasized that the predicted bubble radius should not be interpreted literally, but rather as an index of the decompression stress, similar to the Bubble Grade Index (BGI) introduced by Gernhardt (1991). In fact, the maximum bubble radius predicted by the DCIEM model and the BGI for NoD dives is remarkably similar (Nishi and Tikuisis, 1999). Further, there appears to be a close correlation between R_{max} and the risk of DCS, as presented below.

Model Comparison to DCS Prediction

To substantiate the application of the bubble model to reverse air dive profiles, we first established the correspondence between the predicted maximum bubble size and the risk of DCS. For this purpose, we applied the bubble model to various air and nitrox dives comprising single and repetitive excursions extracted from the recent experimental dive compilation of Temple *et al.* (1999). The selection criterion was arbitrarily based on the maximum DCS incidence for each dive series. Fourteen dive profiles were thus selected and tabled below. The t1 and t2 values correspond to the average of the recorded times when the divers were symptom-free and when symptoms first occurred, respectively. Predictions of R_{max} pertain to the compartment having the larger predicted maximum bubble radius.

Figures 2a - 2d show the predicted N_2 tension and bubble evolution for one profile from each dive type. In these cases, and in most of the profiles tabled above, the predicted time of the maximum bubble radius falls within the t1-t2 envelope. Further, there is a convincing correlation between the predicted risk of DCS and the predicted maximum bubble radius, as seen in Fig. 3. Accordingly, predicted $R_{max} > 60$ μm correspond to pDCS > 3%.

Table 2. Dive profiles and model predictions: Dive Type, sa = single air, sna = single non-air, ra = repetitive air, and rna = repetitive non-air; Dive Series, Profile Notation and Profile # are from Temple *et al.* (1999); pDCS = predicted risk of DCS from USN93 model (courtesy of K.A. Gault, NEDU); n = number of DCS occurrences; t1 = average of last symptom-free time; t2 = average of earliest time of symptom; t_{max} = average time of predicted maximum bubble radius; and R_{max} = predicted maximum bubble radius.

Dive Type	Dive Series	Profile Notation	Profile #	pDCS (%)	n	Depth (fsw)	Time (min)	t1 (min)	(min)	t_{max} (min)	R_{max} (μm)
sa	DC4D	DR0340A	133	6.2	3	148.0	40.0	150.3	280.9	255.0	66.9
	EDU885A	AN1013.OUT	22	7.0	3	60.0	182.7	283.7	403.9	400.0	74.0
	EDU849LT2	EDU849.DAT	43	5.2	19	150.0	30.0	64.8	143.5	98.4	61.1
	NMR97NOD	SIMPLIFIED	2	3.8	7	40.0	200.0	245.4	369.4	350.7	64.5
	EDU545	11/06/44 EDU	1	9.5	12	100.0	85.0	159.0	443.3	276.0	78.2
	PASA	PAA0E04	6	4.6	3	101.5	59.9	274.3	814.3	317.3	60.0
	EDU1157	EDU1157N	14	30.3	4	140.0	240.0	661.3	1025	726.3	103
sna	NMR8697	DRA4_8301	6	1.9	3	71.0	30.0	131.5	271.5	85.5	41.3
	EDI1180S	DIV562	7	10.4	3	150.0	72.3	220.5	401.7	324.4	87.4
ra	PAMLA	PAA1B01	2	10.1	2	81.5	240.1	411.8	651.8	451.1	78.6
	EDU885AR	AN2011.OUT	6	12.9	2	150.0	43.9	519.1	1092	227.7	62.8
	EDU657	11/20/56	42	22.4	2	140.0	60.0	467.6	621.6	501.4	85.0
rna	EDI184	MDC024.OUT	11	9.0	2	80.0	47.4	319.1	370.2	513.5	59.8
	PAMLAOS	PAAIIA03	6	7.4	3	81.5	242.9	497.1	546.1	514.2	71.0

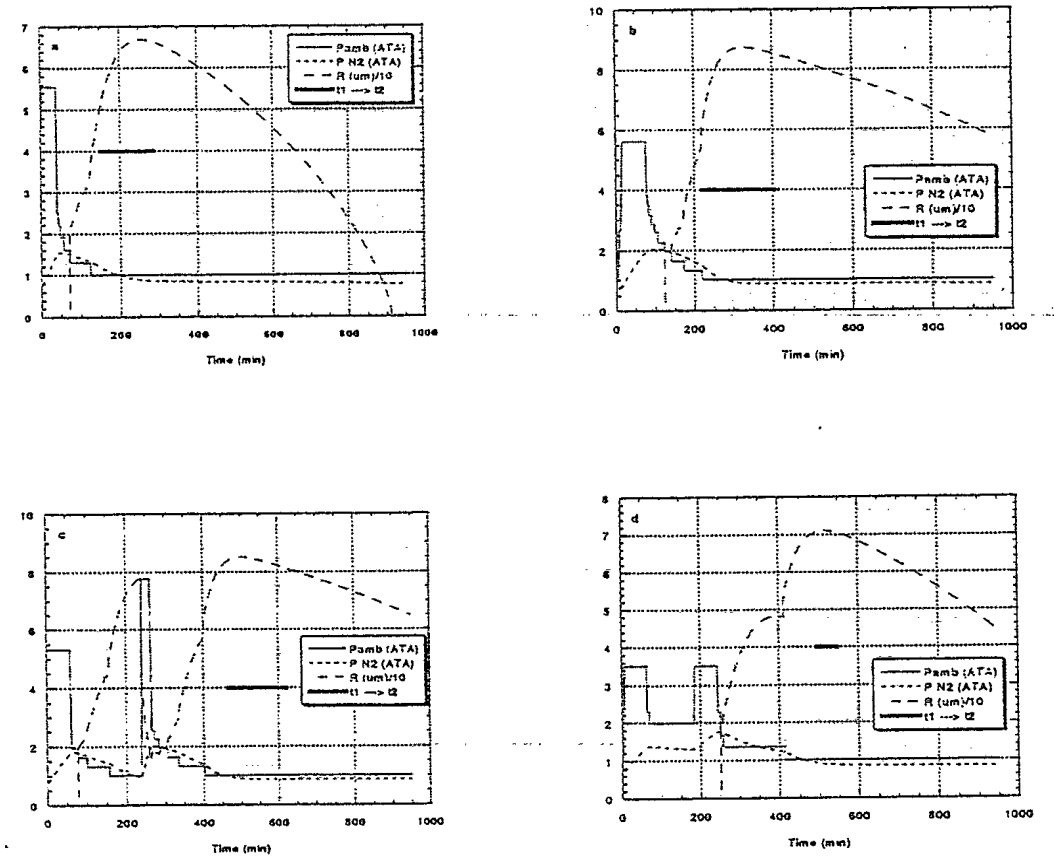

Fig. 2. Predicted N_2 tension and bubble size for dives a) DR4D, b) EDU1180S, c) EDU657, and d) PAMLAOS. The t2→t2 time bar represents the average recorded times between no symptoms and the occurrence of symptoms (see Table 2 for details).

Figure 2c is of particular interest since it represents one of the few reverse dive profiles available in the compilation record (Temple *et al.*, 1999). In this isolated case, the predicted R_{max} is 85.0 µm and pDCS is 22.4% with a 95% confidence interval of 18.5 - 26.1%.

Discussion

The bubble evolution model was developed with close adherence to the physical laws of gas kinetics and the conservation of mass, and most of the resultant parameter estimates are reasonable. Assuming that bubble size is a valid indicator of decompression stress, there is no fundamental reason why the model cannot be applied to reverse dive profiles, nor any reason why the predictions should be interpreted differently from those for normal dives. Further, the model is intuitively appealing since bubble size is particularly sensitive to pressure changes. This aspect may be especially important when comparing the effects of a large pressure change imposed by a reverse dive profile versus a more modest change with a shallower repetitive dive (see Nishi and Tikuisis for detailed examples).

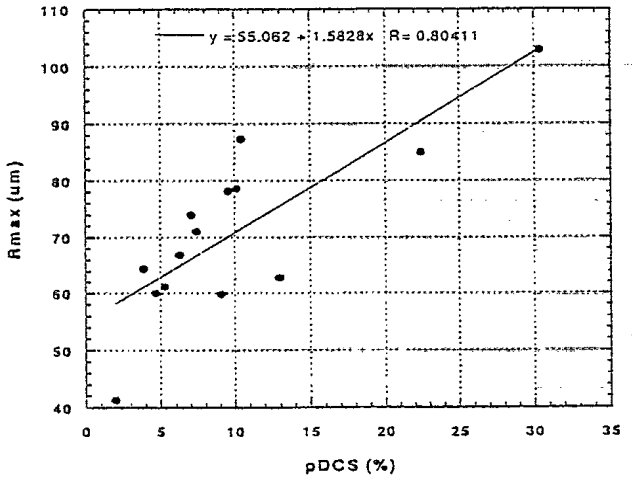

Fig. 3. Comparison of the bubble model prediction of maximum size and the USN93 model prediction of the risk of DCS (see Table 2 for details).

Comparisons of the bubble model predictions to DCS risk predictions suggest that a predicted R_{max} value > 60 µm is associated with a 3% risk of DCS. We conclude that this association can be used to judge the severity of decompression stress for dives within the range of those examined herein, whether normal or reversed.

Literature Cited

Gault, K.A., P. Tikuisis, and R.Y. Nishi. 1995. Calibration of a bubble evolution model to observed bubble incidence in divers. Undersea Hyperbaric Med. 22(3): 249-262.

Gernhardt, M.L. 1991. Development and evaluation of a decompression stress index based on tissue bubble dynamics. Ph.D. Thesis, University of Pennsylvania, Philadephia, Pennsylvania.

Nishi, R.Y. 1993. Doppler and ultrasonic bubble detection. *In:* Bennett, P.B. and D.H. Elliott (eds.). The Physiology and Medicine of Diving. W.B. Saunders, London. Pp. 433-453.

Nishi, R.Y., P. Tikuisis, S.S. Survanshi, E.C. Parker, R. Ball, and P.K. Weathersby. 1997. A comparison of probabilistic models of decompression based on DCS and VGE. Undersea Hyperbaric Med. 24(Supplement): 29.

Nishi, R.Y. and P. Tikuisis. 1999. Development of decompression tables and models: Statistics and data analysis. J Human-Environ. System 2(1): 19-31.

Temple, D.J., R. Ball, P.K. Weathersby, E.C. Parker, and S.S. Survanshi. 1999. The dive profiles and manifestations of decompression sickness cases after air and nitrogen-oxygen dives. NMRC 99-02 (Vols. 1 & 2), Bethesda, Maryland.

#513095